Published in final edited form as:
Mol Cancer Res. 2012 September ; 10(9): 1147–1157. doi:10.1158/1541-7786.MCR-12-0022.

INHIBITION OF THE HEDGEHOG PATHWAY TARGETS THE TUMOR-ASSOCIATED STROMA IN PANCREATIC CANCER

Rosa F. Hwang[1,*], **Todd T. Moore**[1], **Maureen Mertens Hattersley**[2], **Meghan Scarpitti**[2], **Bin Yang**[2], **Erik Devereaux**[2], **Viji Ramachandran**[3], **Thiru Arumugam**[3], **Baoan Ji**[3], **Craig D. Logsdon**[3], **Jeffrey L. Brown**[2], and **Robert Godin**[2]

[1]Department of Surgical Oncology, The University of Texas MD Anderson Cancer Center, Houston, Texas

[2]AstraZeneca Pharmaceuticals, Waltham, Massachusetts

[3]Department of Cancer Biology, The University of Texas MD Anderson Cancer Center, Houston, Texas

Abstract

The Hedgehog (Hh) pathway has emerged as an important pathway in multiple tumor types and is thought to be dependent on a paracrine signaling mechanism. The purpose of this study was to determine the role of pancreatic cancer-associated fibroblasts (human pancreatic stellate cells, HPSCs) in Hh signaling. In addition, we evaluated the efficacy of a novel Hh antagonist, AZD8542, on tumor progression with an emphasis on the role of the stroma compartment.

Expression of Hh pathway members and activation of the Hh pathway were analyzed in both HPSCs and pancreatic cancer cells. We tested the effects of SMO inhibition with AZD8542 on tumor growth *in vivo* using an orthotopic model of pancreatic cancer containing varying amounts of stroma.

HPSCs expressed high levels of SMO receptor and low levels of Hh ligands, whereas cancer cells showed the converse expression pattern. HPSC proliferation was stimulated by sonic Hedgehog with upregulation of downstream GLI1 mRNA. These effects were abrogated by AZD8542 treatment. In an orthotopic model of pancreatic cancer, AZD8542 inhibited tumor growth only when HPSCs were present, implicating a paracrine signaling mechanism dependent on stroma. Further evidence of paracrine signaling of the Hh pathway in prostate and colon cancer models is provided, demonstrating the broader applicability of our findings.

Conclusion—Based on the use of our novel human derived pancreatic cancer stellate cells, our results suggest that Hh-targeted therapies primarily affect the tumor-associated stroma, rather than the epithelial compartment.

Keywords

Pancreatic cancer; Tumor-stromal cell interactions; pancreatic stellate cells; Hedgehog

Address Correspondence To: Rosa F. Hwang, M.D., Associate Professor, Department of Surgical Oncology, The University of Texas MD Anderson Cancer Center, P.O. Box 301402, Unit 444, Houston TX 77230-1402, Tel. 713-563-1873, Fax 713-745-1462, rhwang@mdanderson.org.

Disclosure of Potential Conflicts of Interest: MMH, MS, BY, ED, JLB, and RG are employees of AstraZeneca.

INTRODUCTION

The Hedgehog (Hh) pathway is an essential developmental pathway involved in regulating key aspects of embryogenesis, stem cell maintenance, and tumor biology (1). In humans, the Hh ligands Sonic, Indian, and Desert Hedgehog (SHH, IHH, and DHH) bind to the Patched 1 protein (PTCH1) on target cells, which results in the release of inhibition of the Smoothened (SMO) receptor. SMO is a 7-transmembraneG-protein coupled receptor-like protein that, when activated, results in activation of GLI transcription factors and expression of downstream targets GLI1, PTCH, BCL2, myc, and IGF2.

Aberrantly activated Hh has recently been identified in several malignancies, including basal cell carcinomas (2–4), medulloblastomas (5, 6), lung cancer (7–9), prostate cancer (10–12), and gastrointestinal malignancies (10, 13). In pancreatic adenocarcinoma (PDAC), the Hh pathway is considered one of the “core” signaling pathways that is altered, and the majority of these cancers show abnormal expression of SHH, PTCH1, and SMO (14). Moreover, these factors are expressed early in preneoplastic pancreatic intraepithelial neoplasia (Pan IN) lesions, whereas they are absent in normal pancreatic tissue, suggesting that these factors are important for early tumorigenesis. Blockade of Hh with SMO inhibitors such as cyclopamine inhibited invasion and metastasis and prolonged survival in mouse models of pancreatic cancer (15–17).

Recently, intriguing evidence has emerged suggesting that the Hh pathway is highly active in a paracrine signaling manner in the tumor microenvironment of some pancreatic tumors. When SMO was genetically ablated in the pancreatic epithelium of PDAC-susceptible mice, development of PDAC tumors was not affected, suggesting that Hh signaling in PDAC does not occur in an autocrine manner (18). Using human-tumor xenograft models, Yauch *et al.* (19) used species-specific expression profiling to demonstrate that Hh pathway antagonist treatment resulted in downregulation of Hh target genes only in the murine stromal microenvironment but not within the human tumor epithelial compartment. Similarly, expression of SMO in mesenchymal cells, but not epithelial cells, in the pancreas led to Hh pathway activation, further supporting a paracrine model of Hh-mediated tumorigenesis (20). Finally, treatment of a genetically engineered mouse model of PDAC with the Hh inhibitor IPI-926 resulted in depletion of desmoplastic stroma in pancreatic tumors (21). These observations are consistent with a model in which tumor cells produce Hh ligands that trigger signaling in the stromal microenvironment in a paracrine manner.

Despite these initial observations, the precise role of stromal cells in Hh signaling in pancreatic cancer is not well understood. We have previously shown that the cancer-associated fibroblasts in PDAC (human pancreatic stellate cells, HPSCs) produce secreted factors that promote tumor progression and metastasis *in vitro* and *in vivo* (22). In this study, we analyzed the role of human pancreatic stellate cells (HPSCs) from the tumor-associated stroma in Hh signaling. In addition, we evaluated the efficacy of a novel SMO inhibitor (AZD8542) on pancreatic tumor progression with an emphasis on the role of the HPSCs from the stroma. We present data that strongly suggests the primary mechanism of action of Hh signaling in PDAC occurs in a paracrine manner with ligand expression by the cancer cells and activation of SMO on neighboring HPSCs in the stromal microenvironment.

Materials and Methods

Cell culture

NIH-3T3, human embryonic palatal mesenchyme (HEPM), C3H10T1/2, HeLa, and human colon cancer Colo205 cells as well as BxPC3, Panc1, SU86.86, MiaPaca2, and Capan2 pancreatic cancer cell lines were obtained from American Type Culture Collection (ATCC,

Manassas, VA). Human pancreatic cancerMPanc96 and human pancreatic ductal epithelial (HPDE) cells were obtained from Dr. Timothy J. Eberlein (Washington University, St. Louis, MO) and Dr. M. Tsao (Ontario Cancer Institute, Toronto, Ontario, Canada), respectively. L3.6pl cells were obtained from Dr. I. Fidler (23), and immortalized HPSCs were isolated as previously described (22). Primary human pancreatic stellate cells (HPSCs) were established and cultured as previously described. (22)Both immortalized (using hTERT and SV40T) and non-immortalized primary cells were used in these studies. NIH-3T3, HeLa, pancreatic carcinoma cells, and HPSCs were cultured in Dulbecco's minimal essential medium (DMEM) with 10% FBS (Invitrogen, Carlsbad, CA) and 1% L-glutamine. HEPM and C3H10T1/2 cells were cultured in Eagle's minimal essential medium (EMEM) with Earle's BSS + 2 mM L-glutamine+ 1.0 mM nonessential amino acids+ 1.5 g/L sodium bicarbonate + 10% FBS. HPDE cells were cultured in keratinocyte serum-free media containing 50 μg/mL bovine pituitary extract and 0.2ng/mL recombinant epidermal growth factor (all from Invitrogen). Colo205was maintained as an adherent culture in DMEM containing 10% FBS at 37°C in a humidified atmosphere of 6% CO_2. All other cells were cultured at 37°C in a humidified atmosphere of 5% CO_2.

GLI1reporter assays: Mouse and human versions

A subset of the proprietary AstraZeneca compound collection (40,000 compounds) with similarity to cyclopamine was screened using a GLI1luciferase reporter assay to identify inhibitors of the Hh pathway. (24) The GLI1luciferase construct consists of 8 Gli-binding sites upstream of a luciferase reporter gene (25). The construct was transfected into NIH-3T3 cells along with a constitutively active Renilla luciferase construct as a control. Stable cells were selected and stimulated with 50% SHH-containing conditioned medium. Conditioned media was generated by transfecting HEK293 cells with a SHH expression vector and collecting media 48–96 hours after transfection. Cells were treated with Hh inhibitor compounds (in dimethyl sulfoxide) at varying concentrations for 24 hours and assayed for luciferase activity using the Dual-Glo Luciferase Assay System (Promega, Madison, WI) per the manufacturer's instructions. HEPM cells and C3H10T1/2 cells were treated with inhibitor compounds for 24 hours and assayed for luciferase reporter activity using the Steady-Glo Luciferase Assay System (Promega) per the manufacturer's instructions. Plates were read on the Tecan Ultra microplate reader (Tecan, Mannedorf, Switzerland) at50ms integration time per well.

Differentiation assay

To evaluate the efficacy of SMO inhibitor compounds, an osteoblast differentiation assay was performed using C3H10T1/2 cells, which differentiate into osteoblasts after stimulation with SHHor Wnt. In brief, C3H10T1/2 cells were plated into 384-well plates, and media was changed to low serum (2% FBS) or conditioned media containing either SHH or WNT3a. Cells were then treated with inhibitor compounds for 72 hours, and alkaline phosphatase activity was measured. Cells were lysed in 15 μl of 1× RIPA cell lysis buffer, incubated at −80°C for 30 minutes, treated with p-nitrophenyl phosphate at 1 mg/mL in diethanolamine buffer (pH 9.8), incubated at 30°C overnight for color development, and read at absorbance of 405 nm.

SMO Binding Assay

HeLa cells were transfected with pcDNA vector expressing human or mouse myc-tagged SMO (GeneCopoeia, Rockville, MD; FuGENE transfection reagent, Promega). After 24 hours incubation, media was changed to low serum (0.5% FBS). The cells were then pre-treated with various concentrations of SMO inhibitors for 20minutes, followed by3nM BODIPY-labeled cyclopamine (Toronto Research Chemicals, Ontario, Canada) and incubated at 37°C for 4hours. After incubation, the cells were fixed with 3%

paraformaldehyde and 0.5%TritonX +1x PBS (Invitrogen). The cells were then washed, blocked with 10% goat serum (Fisher Scientific, Pittsburgh, PA), and incubated with myc-tagged antibody (Cell Signaling Technology, Beverly, MA) for 2 hours followed by Alexa Fluor 594 anti-rabbit antibody (Invitrogen). Cells were stained with Hoechstdye (Invitrogen), and fluorescence was detected using an ImageXpress system (Molecular Devices, Sunnyvale, CA).

Proliferation Assay

HPSCs were seeded at 2000 cells per well in triplicate in 96-well plates and cultured in DMEM containing 10% FBS. After overnight attachment, media was changed to DMEM containing 1% FBS, and varying concentrations (0, 1.0, 1.5, 2 μg/mL) of recombinant SHH (rSHH, R&D Systems, Minneapolis, MN) were added to the wells. Cell proliferation was analyzed at 72hoursusing MTS reagent (Promega) added 1hourbefore taking a spectrophotometric reading according to the manufacturer's instructions.

Hedgehog Stimulation of HPSCs

HPSCs were seeded in 6-well plates and grown to 70% confluence in DMEM containing 10% FBS. The media was then changed to serum-free DMEM overnight. rSHH or rIHH (R&D Systems) was added to the wells (2 μg/mL) along with varying concentrations (0, 10, 100, 1000nM) of the SMO inhibitor AZD8542 (AstraZeneca). Cells grown in 1% DMEM without rSHH, rIHH or AZD8542served as controls. RNA was isolated after 24 hours, and expression of GLI1 was measured by quantitative reverse transcriptase (RT)-PCR (qRT-PCR) and normalized to HPRT.

Colon cancer subcutaneous xenograft models

Animal protocols for the colon cancer models were approved by the AstraZeneca R&D Bostonsite's Institutional Animal Care and Use Committee. All animal work was conducted in accordance with applicable internal standards and external local and national guidelines, regulations, and legislation. Female Ncr nude mice aged 6 to 8 weeks were maintained under specific-pathogen-free conditions in a facility accredited by the Association for Assessment and Accreditation of Laboratory Animal Care International.

Colo205 cells were implanted subcutaneously in the right flank (4×10^6 cells/mouse) in 0.1 mL of serum-free media. Tumors were allowed to grow until they reached an average volume of 200mm^3, and mice were randomized (N=5/treatment group.) AZD8542was suspended in 0.5% (v/v) hydroxypropyl methyl cellulose (HPMC) in sterile water and administered orally once daily (20 or 40 mg/kg). Tumor and blood samples were collected in RNAlater (Ambion, Austin, TX) and EDTA, respectively, at 1, 4, 6, 8, 12, and 16 hours after dosing. In a co-implantation xenograft model of colon cancer, mice were injected with both HT29 (0.3×10^6) and MEF (1.5×10^6) cells subcutaneously in the right flank (100 μl/injection) for a final tumor: stroma (T/S) ratio of 1:5. When tumors reached 70–100 mm^3, animals were randomized to receive either SMO inhibitor (20–80 mg/kg) or vehicle (0.5% HPMC/0.1% Tween80) (N=10/group). Tumor measurements and body weights were recorded twice weekly. Data are expressed as percentage tumor growth inhibition at day 29. For pharmacodynamic studies, tumors were collected 8 hours after each dose in RNAlater (Qiagen, Germantown, MD) or formalin (Newcomer Supply, Middleton, WI). Blood was collected for pharmacokinetic analysis.

Tumors were lysed using a Lysing Matrix D tube (MP Biomedicals, Solon, OH) with RLT buffer containing 1% b-mercarptoethanol and homogenized with the Fast-Prep-24 Instrument (MP Biomedicals). RNA was isolated using the RNeasy Midi Kit Column (Qiagen) and converted to cDNA using the High-Capacity cDNA Archive Kit (Applied

Biosystems, Foster City, CA). Quantitative RT-PCR was performed using primers for mouse GLI1 (Applied Biosystems) on the 7900HT TaqMan real-time PCR instrument (Applied Biosystems). Data were normalized to housekeeping gene HPRT.

Orthotopic model of pancreatic cancer

All pancreatic cancer animal experiments were reviewed and approved by the MD Anderson Institutional Animal Care and Use Committee. An orthotopic nude mouse model of pancreatic cancer using BxPC3 pancreatic tumor cells labeled with firefly luciferase (BxPC3-FL) has previously been described by this lab (22). All mice were divided into groups with varying tumor/stroma (T/S) ratios with intrapancreatic injections of: (a) 1×10^6 BxPC3-FL cells alone (T/S 1:0), (b) 1×10^6 BxPC3-FL cells and 1×10^6 HPSCs (T/S 1:1), or (c) 1×10^6 BxPC3-FL cells and 3×10^6 HPSCs (T/S 1:3) suspended in 50 μL of HBSS (Sigma Aldrich, St. Louis, MO). Groups were further subdivided into those treated with AZD8542and those receiving vehicle only. Treatment with 80mg/kg AZD8542suspended in 200 μL of vehicle—0.5% (hydroxypropyl) methyl cellulose (Sigma Aldrich) with 0.1% Tween 80 (Fisher Scientific)—or with vehicle alone was administered daily by oral gavage starting on day 4 after tumor implantation. Bioluminescence imaging was performed twice weekly to assess the luciferase signal from BxPC3 cells using the IVIS imaging system (Caliper Life Sciences, Hopkinton, MA)(22). Mice were euthanized, and tumors were harvested, measured and either snap-frozen or fixed in formalin for further processing. The same experiment was performed using MPanc96-FLcancer cells.

Immunohistochemistry

Briefly, for Ki67 staining, formalin-fixed paraffin embedded slides were deparaffinized in xylene, rehydrated and blocked with 3% H_2O_2. Antigen retrieval was performed by steaming in antigen unmasking solution (Vector Lab, Burlingame CA). Slides were blocked with 4% fish gelatin and incubated overnight with rabbit anti-Ki67 antibody (1:300; Fisher, Pittsburgh PA) at 4°C and washed with PBS. After incubation with biotinylated goat anti-rabbit IgG (Vector Lab) for1hr at room temperature, slides were washed and Incubated for 30 minutes with VECTASTAIN® ABC Reagent (Vector Lab). A positive reaction was detected by exposure to stable 3,3′-diaminobenzidine (Trevigen, Gaithersburg MD) for 10–20min. Slides were counterstained with Gill's hematoxylin. The Aperio ScanScope CS Slide Scanner (Aperio Technologies, Vista CA) was used to digitally scan the slides with a 20X objective and images were analyzed using Aperio Imagescope software for nuclear staining with Ki67.

For CD31 staining, frozen slides were fixed in cold acetone and endogenous peroxidase was blocked with 3% H_2O_2. Slides were blocked with 5% normal horse serum + 1% normal goat serum in PBS, incubated with rat anti-mouse CD31 antibody (1:50; BD PharMingen) at room temperature for 2 hours and washed with PBS. After incubation with peroxidase-AffiniPure goat anti-rat IgG (1:200; Jackson) for 1 hr at room temperature, a positive reaction was detected by exposure to stable 3, 3′-diaminobenzidine (Trevigen, Gaithersburg MD) for 5 minutes. Nuclei were counterstained with Gill's hematoxylin.

Quantitative RT-PCR

RNA was isolated from homogenized snap-frozen tumor tissue and cultured cell lines using TRIzol (Invitrogen) according to the manufacturer's instructions. cDNA was made from RNA using the QuantiTect Reverse Transcription System kit (Qiagen) according to the manufacturer's instructions. qPCR for SMO, SHH, PTCH1, GLI1, and HPRT (Applied Biosystems) was performed using TaqMan gene expression assays (Applied Biosystems) according to the manufacturer's specifications. Quantification was accomplished using the

standard curve method. qPCR was also performed for GLI1 in HPSCs labeled with green fluorescent protein (HPSC-GFP) with or without co-culture with BxPC3 cells for 96 hours.

Western blotting

Cell lysates were prepared from HPSC and pancreatic cancer cells and protein concentrations were measured by BioRad reagent. Protein (40 ug) was loaded onto 10% SDS-PAGE gels and Western blotting was conducted using a rabbit primary antibody against SHH or IHH (Cell Signaling) at a 1:1000 dilution and goat anti-rabbit secondary antibody (LiCor, Lincoln NE) at a 1:10,000 dilution. Blots were re-probed for β-Actin (1:1000 dilution; Abcam, Cambridge MA), which served as loading control.

Statistical analysis

Experiments were done in triplicate and representative data are shown. Statistical analysis was done using GraphPad Prism software (GraphPad, San Diego, CA). Comparisons were made using the two-tailed Student's *t* test, and significant difference was defined as $P < 0.05$. Data are shown as mean ± SEM.

RESULTS

Identification of potent Hedgehog pathway inhibitors

Screening of the AstraZeneca compound library using a GLI1luciferase reporter assay identified several compounds with an IC50 of <10nM (Supplemental Figure 1A) and no activity against the control Renilla vector. To show specificity of the compounds for the Hh pathway, we utilized an osteoblast differentiation assay stimulated by 2different ligands known to act at different points in the differentiation process. After stimulation with conditioned media containing either SHH or Wnt3A, mouse C3H10T1/2 cells were analyzed for secreted alkaline phosphatase as an indicator of osteoblast differentiation. Several compounds were identified to have an IC50 of <20nM with SHH stimulation (Supplemental Figure 1), but none were shown to inhibit osteoblast differentiation when stimulated with Wnt3a (data not shown), indicating the specificity of the compounds for the Hh pathway. None of the compounds identified were able to inhibit proliferation in a panel of 60 tumor cell lines, consistent with previous reports (19, 26). The most promising clinical candidate was AZD8542 (Figure 1A).

AZD8542bindsSMO and inhibits Hh pathway signaling

To determine whether the inhibitors acted specifically on SMO, we used a cyclopamine displacement assay. HeLa cells engineered to express either human or mouse SMO were pre-treated with SMO inhibitor compounds, followed by cyclopamine labeled with BODIPY. To validate the assay, unlabeled KAAD-cyclopamine was used as a competitor for BODIPY-labeled cyclopamine; it showed a similar affinity for both mouse and human SMO (2nM vs. 0.8nM, data not shown). Fluorescent images of cells treated with AZD8542 are shown in Figure 1B. In this assay, AZD8542 shows a Kd of 5nMfor mouse SMO and a Kd of 20nM for human SMO, indicating that the compound has a similar range of affinity for both mouse and human SMO (Figure 1C).

Furthermore, we tested the ability of AZD8542 to not only bind SMO but also block downstream GLI1signaling in both mouse and human cells. C3H10T1/2 (mouse) and HEPM (human) cells expressing GLI1-responsive luciferase reporter genes were stimulated with SHH conditioned media and treated with AZD8542. AZD8542 was able to effectively inhibit GLI1activity with an IC50 of 2.9 nM in the mouse cell line and an IC50 of 0.02 nM in the human cell line, indicating increased potency against the human reporter line (Supplemental Figure 1B). These data establish that AZD8542 is an ideal candidate to

evaluate effects on the Hh pathway in models containing both human and mouse components.

Expression of the Hedgehog pathway in pancreatic cancer and stromal cells

A panel of cells including pancreatic cancer, normal pancreatic duct, and HPSCs from PDAC were analyzed for expression of genes involved in the Hh pathway (Figure 2). SMO was expressed at high levels in HPSCs and at lower levels in all other cancer cells tested. The expression level in a few cancer cells (SU86.86, MiaPaca2, and Capan2) was moderate (Figure 2A). In contrast, the SHH ligand was absent in HPSCs but was expressed in several cancer cell lines (Panc1, MPanc96, Capan2; Figure 2Band Supplemental Figure 2A). Similarly, IHH was expressed in cancer cells BxPC3 and MPanc96 but not HPSCs (Supplemental Figure 2A). The downstream targets PTCH1 and GLI1 were expressed in both cancer and stellate cells to varying degrees (Figure 2C–D). To confirm the generalizability of these results to other HPSC cell lines, we analyzed the expression of SMO, SHH, PTCH1, and GLI1 in primary HPSCs (non-immortalized) obtained from 3unique patients and found that expression levels of these genes were similar to those of the HPSC cell line used in these studies (data not shown).

SHH-mediated stimulation of HPSCs is inhibited by AZD8542

Others have shown that activation of the Hh pathway by rSHH does not affect endogenous GLI1messenger levels in tumor epithelial cells (Bxpc3 and CFPAC-1), regardless of SMO expression in these cells (19). However, it has been suggested that Hh signaling acts in a paracrine fashion because SMO inhibition in the mouse stroma of xenograft tumor models is required for growth inhibition (19). We determined the effects of Hh pathway activation in HPSCs by evaluating cell proliferation, migration, and GLI1expression. Treatment of HPSCs with rSHH (1.5 and 2.0 μg/mL) resulted in increased cell proliferation with a peak effect of 173.1% of control ($p<0.005$; Figure 3A). Accordingly, downstream GLI1expression also increased with rSHH stimulation (5.7-fold vs. control, $p<0.05$; Figure 3B). Inhibition of SMO by AZD8542 effectively abrogated the rSHH-mediated induction of GLI1at 100–1000 nM (0.25–0.5-fold vs. control, $p<0.05$). Similar results were obtained in a human prostate stromal cell line (Supplemental Figure 1B). Although rSHH stimulated HPSC activity, it had no effect on pancreatic cancer cell (Bxpc3 and Panc1) proliferation or migration (data not shown). HPSCs also responded to IHH treatment with increased cell proliferation and increased levels of GLI1mRNA (Supplemental Figure 2).

AZD8542 inhibits the Hh pathway in an in vivo colon cancer model

Although AZD8542 showed potent inhibition of Hh *in vitro*, we wanted to test the ability of the compound to affect the Hh pathway *in vivo*. Initially, we used a Colo205 xenograft model, which expresses SHH ligand in the tumor cells but no IHH ligand (Supplemental Figure 4A). Using species-specific primers, we observed strong inhibition of GLI1only in the mouse stromal compartment but not the human epithelial compartment (Supplemental Figure 4B). GLI1inhibition was time dependent, with maximum inhibition at 8 hours after dosing and recovery by 16 hours. Plasma levels of AZD8542 were significant (60 μg/mL) at 1 hour after dosing, with depletion by 8 hours (Supplemental Figure 4C). Interestingly, this time frame corresponds to the time required for maximum GLI1inhibition, indicating a 6-hour time delay between SMO inhibition and the effect on GLI1transcription. These data show that AZD8542 is orally available and able to inhibit the Hh pathway in the stromal component of the Colo205 xenograft model.

Although AZD8542 was able to inhibit Hh signaling in the Colo205 model, we observed no effect on tumor growth. Thus, we used a co-implant model with a different colon cancer cell line, HT29, known to express SHH combined with mouse embryonic fibroblasts (MEFs)—

cells known to be highly responsive to the Hh pathway (19). Animals treated with 80 mg/kg AZD8542 showed significant tumor growth inhibition of 79% compared to vehicle controls ($p<0.001$; Supplemental Figure 5A). The effect on tumor growth was dose dependent, with 52% and 46% tumor inhibition at 40 and 20 mg/kg, respectively ($p<0.001$ and $p<0.005$; Supplemental Figure 5A). The compound was well tolerated, with no significant changes in body weight (not shown). Accordingly, AZD8542 treatment resulted in a dose-dependent decrease in mouse GLI1 and PTCH1expression in tumors, with nearly complete abrogation of expression at the highest dose (Supplemental Figures4B and 5B). Plasma levels of AZD8542 increased with each higher dose (Supplemental Figure 5C), peaking at 30 μg/mL ± 12.6 with the most effective dose for tumor inhibition (80 mg/kg). To further investigate the effect of AZD8542 on the stromal compartment, we analyzed tumors for alpha smooth muscle actin (αSMA) expression. Tumors treated with AZD8542 expressed markedly less αSMA than did the control group (Supplemental Figure 5D), suggesting that AZD8542 acts primarily on the tumor-associated stroma rather than the epithelial compartment in this model.

Treatment with AZD8542 reduces growth of pancreatic tumors and metastases

Having established that AZD8542 is able to inhibit tumor growth in the stromal-dependent HT29/MEF model, we wanted to evaluate the effects of Hh pathway inhibition in a more clinically relevant model containing a human stromal component. We have previously shown that co-injection of HPSCs with cancer cells results in significantly increased pancreatic tumor growth and metastasis in a mouse model (22). After observing that AZD8542 abrogated rSHH-mediated stimulation of GLI1expression in HPSCs, we sought to determine the *in vivo* effects of AZD8542 on pancreatic cancer growth and metastasis in our co-injection model of PDAC. Mice were injected in the pancreas with Bxpc3 cells labeled with firefly luciferase (Bxpc3-FL) and HPSCs in T/S ratios of 1:0, 1:1, or 1:3. Four days after cells were injected, mice began treatment with AZD8542 (80 mg/kg oral gavage daily) or vehicle alone. Tumor growth was followed in real time using IVIS imaging. Mice were euthanized on day 32 of treatment.

In the group of mice with Bxpc3 alone without HPSCs (T/S ratio of 1:0), treatment with AZD8542 had no significant effect on tumor growth (data not shown). However, AZD8542 treatment of mice with a T/S ratio of 1:3 resulted in reduced growth of the pancreatic tumors beginning after day 15 of treatment and reached statistical significance at day 30 (Figure 4A). The final volume of pancreatic tumors after completion of AZD8542 treatment was significantly lower in the group of mice with a T/S ratio of 1:3 compared to the volume in mice with vehicle treatment alone ($1054\ mm^3 \pm 224$ vs. $4629\ mm^3 \pm 1450$, $p=0.04$; Figure 4B). Although tumors in the T/S 1:1 group were smaller with AZD8542 treatment than those in the vehicle control group, this difference did not reach statistical significance (Figure 4B and Supplemental Figure 6). Furthermore, expression of downstream GLI1and PTCH1was significantly reduced specifically in the stromal component of tumors treated with AZD8542 in the groups with a T/S ratio of 1:3 (Figure 4C–D), indicating that the Hh pathway was inhibited. However, these markers were not significantly affected in the groups with T/S ratios of 1:0 or 1:1 (data not shown). To confirm whether BxPC3 directly activates Hedgehog signaling in HPSCs, HPSCs labeled with GFP were cultured with BxPC3 for 96 hours and sorted by flow cytometry. Gli1 expression was significantly increased in HPSCs after co-culture with BxPC3 cells compared to controls (Figure 5A), indicating that BxPC3 cells do indeed activate the Hh pathway in HPSCs.

Additional analysis was performed to elucidate whether SMO inhibition affected cancer or stromal cell proliferation and tumor vascularity. Expression of Ki67 was reduced significantly in the tumors of mice with T/S ratio 1:3 treated with AZD8542 compared to controls (71.9 ± 1.9 vs. 42.2 ± 4.4, $p<0.005$, Figure 5B). The Ki-67 positive cells were

primarily in areas of cancer, not stroma, indicating that SMO inhibition affected proliferation of primarily cancer cells but not stellate cells. There was no difference in Ki67 expression in tumors derived from lower amounts of stroma. Tumor vascularity in the T/S 1:3 group was increased with AZD8542 treatment by CD31 immunohistochemistry (24.2 ± 3.1 vs. 82.6 ± 7.1, $p<0.0001$; Figure 5C).

Mice in the T/S 1:3 group also developed fewer liver metastases with AZD8542 treatment compared to control mice (Figure 6A) with lower luciferase signal (1.86×10^5 vs. 95.9×10^5 photons, $p=0.06$), although this difference did not reach statistical significance. Metastatic lesions were confirmed histologically (Figure 6B). Careful examination by IVIS imaging and gross examination did not reveal a significant volume of other metastatic lesions (e.g.-lung, retroperitoneum) other than the liver. Similar to our observations with primary pancreatic tumors, AZD8542 treatment had no effect on liver metastases in the groups with T/S ratios of 1:0 or 1:1 (data not shown). Serial IVIS imaging suggests that the effect of AZD8542 was to inhibit tumor seeding at sites of distant metastasis, rather than to inhibit the expansion of metastatic lesions (Supplemental Figure 7). Unlike mice in the control group, mice in the drug treatment group did not develop a signal outside the pancreas.

DISCUSSION

In the present study, our results suggest that Hh signaling occurs in a paracrine fashion that is dependent on activation of SMO on neighboring pancreatic stellate cells in the tumor microenvironment of pancreatic cancer. Furthermore, we describe the development of a novel Hh antagonist that potently binds SMO and affects the tumor-associated stroma in mouse models of cancer, resulting in inhibition of tumor growth and metastasis.

Expression of Hh pathway components revealed that SMO and GLI1were primarily observed in stromal-derived HPSCs, whereas the ligands SHH and IHH were limited to pancreatic tumor cells, suggesting a paracrine signaling mechanism. In support of this, treatment of HPSCs with SHH and IHH activated the Hh pathway, as measured by upregulation of GLI1mRNA, and stimulated the proliferation of HPSCs. This effect was blocked by the SMO inhibitor AZD8542. No effect of SHH stimulation or SMO inhibition was observed on pancreatic cancer cell activity.

Although previous reports have suggested a possible autocrine role for Hh signaling, the concentration of Hh antagonist required to downregulate the Hh pathway in cancer cells was significantly higher (1.9 μM-6 μM)(15, 19) than the effective dose in our studies (10–100 nM). Our data correlate with observations by Yauch *et al.* (19), who found that the IC50of Hh antagonist to inhibit growth of a mesenchymal cell line was 400 times lower than that required for the most sensitive cancer cell line (5 nM vs. 1.9 μM). High concentrations of Hh antagonist resulted in repression of unrelated transcriptional reporters, suggesting that previously observed effects in cancer cells may be due to off-target effect (19).

Using *in vivo* models of colon cancer and pancreatic cancer, we show that AZD8542 inhibits the Hh pathway specifically in the stromal compartments of each model. In the Colo205 colon xenograft model, species-specific RT-PCR showed strong inhibition of GLI1in the mouse stromal compartment but no downregulation in the human epithelial compartment. No effect on tumor growth inhibition was observed. However, in both the HT29/MEF and BxPC3/HPSC orthotopic pancreatic cancer models, AZD8542 significantly reduced tumor growth. Interestingly, growth inhibition was observed only when tumors contained both stromal cells and cancer cells but not cancer cells alone. Moreover, downstream Hh signaling in both tumor models was inhibited by AZD8542. Although the

BxPC3 cells used in the orthotopic pancreatic cancer model shown in Figure 4 do not express appreciable levels of SHH, they do express IHH which has similar effects on HPSCs as does SHH (Supplemental Figure 2). Thus, IHH is most likely the ligand participating in Hh signaling in the BxPC3 orthotopic model. In addition, we have performed the same experiment using MPanc96, which expresses high levels of SHH, with similar effects of AZD8542 on tumor growth inhibition (Supplemental Figure 3). Taken together, these results indicate that SMO inhibition blocks Hh signaling in the stromal compartment, resulting in an overall reduction in tumor growth and metastasis. Our data support several recent reports showing that Hh ligands are expressed by epithelial cells, which in turn activate Hh signaling in the adjacent stroma with the overall effect of promoting tumor growth (18–20). Activation of the Hh pathway by expression of mutant SMO (SMOM2) specifically in pancreatic ductal epithelial cells driven by PDX promoter did not initiate tumorigenesis. In these genetically engineered mice, Hh signaling was active in mesenchymal cells but not neoplastic pancreatic epithelial cells (20). Furthermore, species-specific qRT-PCR analysis of primary human tumor xenografts showed correlation between SHH and IHH expression in the tumor and activation of GLI1in the stromal compartment (19). Finally, analysis of microdissected samples of human PDAC showed that the levels of Hh ligand (SHH and IHH) were significantly higher in the tumor epithelial cells than in stromal cells, whereas GLI1was much higher in tumor stroma (20).

To our knowledge, the current study is the first to investigate Hh signaling using primary HPSCs derived from PDAC. The precise mechanism by which Hh signaling in HPSCs promotes pancreatic tumor growth and metastasis is unknown. We have shown that conditioned media from activated HPSCs stimulates pancreatic tumorigenesis *in vitro* and *in vivo*. It is likely that Hh ligand secreted from neighboring cancer cells stimulates HPSCs to produce soluble factors that then feed back on cancer cells to promote their activity. Expression profiling of tumor xenografts treated with Hh antagonist showed repression of the Wnt pathway and insulin-like growth factor receptor in the mouse stroma (19).

Inhibition of tumor growth in the PDAC/HPSC co-injection model with AZD8542 was associated with decreased cancer cell proliferation and increased vascularity. We did not see an obvious difference in stellate cell proliferation or stroma formation in these tumors and yet our data indicate that SMO inhibition with AZD8542 promotes the activity of stellate cells, not pancreatic cancer cells. It is plausible that SMO inhibition may have act directly on HPSCs to alter the nature of their secreted factors, which in turn indirectly acts on cancer cells in a paracrine manner to result in overall tumor inhibition. Although our observation of increased angiogenesis with SMO inhibition correlates with studies by Olive *et al.* using a genetically engineered mouse model of PDAC (21), a recent report by Chen *et al.* demonstrated a pro-angiogenic role of Hh signaling (27). Treatment of a colorectal cancer xenograft model with another SMO inhibitor resulted in decreased vascularity. (27) These observations appear to be contradictory and thus, additional studies to elucidate the effects of Hh signaling on pancreatic stellate cells and angiogenesis are currently in progress.

Another potential mechanism by which Hh signaling in the stroma might regulate both tumor growth and chemosensitivity is through the promotion of cancer stem cell-like properties. Several investigators have demonstrated the role of Hh signaling in regulating cancer stem cell renewal in breast cancer, gliomas, and leukaemia (28–31). Cells that undergo epithelial-mesenchymal transition (EMT) have many properties of cancer stem cells, such as self-renewal and resistance to toxic injuries, including chemoradiation. Although pancreatic stellate cells have not clearly been shown to participate in cancer stem cell renewal, they do promote EMT changes in pancreatic cancer cells (32). Thus, Hh signaling in HPSCs might also affect stem cell properties in PDAC with an overall effect of increased tumorigenesis as well as resistance to chemotherapy.

In PDAC and other solid malignancies, the tumor-associated stroma has been implicated as a physical barrier to the delivery of chemotherapy (33). The effects of Hh blockade on chemoresistance were not studied in this paper but have been described previously by others. Using a genetically engineered mouse model of PDAC that develops extensive stroma, Olive *et al.* (21) demonstrated improved efficacy of gemcitabine when combined with an Hh antagonist. Tumors in this model are poorly perfused, which hampers the delivery and efficacy of gemcitabine treatment. However, treatment with an Hh antagonist depleted tumor-associated stroma and improved tumor vascularity, increased intratumoral concentration of gemcitabine, and stabilized disease (21). In support of those findings, we have shown in our HT29/MEF model a reduction of αSMA staining upon treatment with AZD8542. Not only does stroma act as a physical obstacle to delivery of chemotherapy, but it also inhibits its efficacy on a molecular level. We have shown that conditioned media from HPSCs protects cancer cells from apoptosis induced by chemotherapy or radiation (22), although the precise mechanisms are unclear. Hh signaling has been shown to induce chemoresistance as well as resistance to ionizing radiation (34–36). Therefore, it is possible that activation of Hh signaling in HPSCs may also inhibit neighboring cancer cell responsiveness to chemotherapeutic agents or radiation.

A range of clinical trials targeting the Hh pathway has emerged recently. A Phase II study of the SMO inhibitor vismodegib (Genentech) showed efficacy in objective response rate in patients with basal cell carcinoma, resulting in FDA approval in early 2012. However, a recent Phase II trial by Infinity Pharmaceuticals to evaluate the SMO inhibitor saridegib (IPI-926-03) in combination with gemcitabine in patients with metastatic pancreatic cancer was halted after preliminary analysis showed a difference in survival favoring the placebo plus gemcitabine arm. The reasons for failure are unknown since the full data analysis from this trial has not been published. As demonstrated by our data and others, the efficacy of Hh antagonists in PDAC appears to be dependent on the stromal compartment; whether stroma is a significant component and driving force in metastatic pancreatic cancer is unknown. Perhaps the key to success with Hh inhibitors may be the ability to better select patient populations that have tumors dependent on the stroma and the Hh pathway for growth and maintenance.

In summary, our results are direct evidence of Hh signaling in pancreatic stellate cells in the tumor-associated stroma of pancreatic cancer. Activation of the Hh pathway in PDAC occurs in a paracrine fashion, and disruption of the pathway with a novel SMO antagonist, AZD8542, reduced pancreatic tumor growth and metastasis specifically by inhibiting the stromal compartment. Thus, preclinical cancer models that lack stroma are not adequate tools for testing Hh-targeted therapies.

Supplementary Material

Refer to Web version on PubMed Central for supplementary material.

Acknowledgments

Financial Support: This work is supported by the National Institutes of Health through grant 1K08CA138912-01A1 to RFH and through MD Anderson's Cancer Center Support Grant, 5P30CA016672.

We would like to thank James Janetka, Mukta Bagul, Troy Patterson, Chris Pien, Alex Hird, Les Dakin, Qibin Su, Alex Cao, Patrick Brassil, Dan Russell and Yan Liu for their contributions and support to the project team.

References

1. Ingham PW, McMahon AP. Hedgehog signaling in animal development: paradigms and principles. Genes Dev. 2001; 15:3059–87. [PubMed: 11731473]
2. Green J, Leigh IM, Poulsom R, Quinn AG. Basal cell carcinoma development is associated with induction of the expression of the transcription factor Gli-1. Br J Dermatol. 1998; 139:911–5. [PubMed: 9892966]
3. Xie J, Murone M, Luoh SM, Ryan A, Gu Q, Zhang C, et al. Activating Smoothened mutations in sporadic basal-cell carcinoma. Nature. 1998; 391:90–2. [PubMed: 9422511]
4. Oro AE, Higgins KM, Hu Z, Bonifas JM, Epstein EH Jr, Scott MP. Basal cell carcinomas in mice overexpressing sonic hedgehog. Science. 1997; 276:817–21. [PubMed: 9115210]
5. Berman DM, Karhadkar SS, Hallahan AR, Pritchard JI, Eberhart CG, Watkins DN, et al. Medulloblastoma growth inhibition by hedgehog pathway blockade. Science. 2002; 297:1559–61. [PubMed: 12202832]
6. Rubin JB, Rowitch DH. Medulloblastoma: a problem of developmental biology. Cancer Cell. 2002; 2:7–8. [PubMed: 12150819]
7. Yuan Z, Goetz JA, Singh S, Ogden SK, Petty WJ, Black CC, et al. Frequent requirement of hedgehog signaling in non-small cell lung carcinoma. Oncogene. 2007; 26:1046–55. [PubMed: 16909105]
8. Chi S, Huang S, Li C, Zhang X, He N, Bhutani MS, et al. Activation of the hedgehog pathway in a subset of lung cancers. Cancer Lett. 2006; 244:53–60. [PubMed: 16446029]
9. Watkins DN, Berman DM, Burkholder SG, Wang B, Beachy PA, Baylin SB. Hedgehog signalling within airway epithelial progenitors and in small-cell lung cancer. Nature. 2003; 422:313–7. [PubMed: 12629553]
10. Karhadkar SS, Bova GS, Abdallah N, Dhara S, Gardner D, Maitra A, et al. Hedgehog signalling in prostate regeneration, neoplasia and metastasis. Nature. 2004; 431:707–12. [PubMed: 15361885]
11. Sanchez P, Hernandez AM, Stecca B, Kahler AJ, DeGueme AM, Barrett A, et al. Inhibition of prostate cancer proliferation by interference with SONIC HEDGEHOG-GLI1 signaling. Proc Natl Acad Sci U S A. 2004; 101:12561–6. [PubMed: 15314219]
12. Fan L, Pepicelli CV, Dibble CC, Catbagan W, Zarycki JL, Laciak R, et al. Hedgehog signaling promotes prostate xenograft tumor growth. Endocrinology. 2004; 145:3961–70. [PubMed: 15132968]
13. Berman DM, Karhadkar SS, Maitra A, Montes De Oca R, Gerstenblith MR, Briggs K, et al. Widespread requirement for Hedgehog ligand stimulation in growth of digestive tract tumours. Nature. 2003; 425:846–51. [PubMed: 14520411]
14. Thayer SP, di Magliano MP, Heiser PW, Nielsen CM, Roberts DJ, Lauwers GY, et al. alHedgehog is an early and late mediator of pancreatic cancer tumorigenesis. Nature. 2003; 425:851–6. [PubMed: 14520413]
15. Feldmann G, Dhara S, Fendrich V, Bedja D, Beaty R, Mullendore M, et al. Blockade of Hedgehog Signaling Inhibits Pancreatic Cancer Invasion and Metastases: A New Paradigm for Combination Therapy in Solid Cancers. Cancer Res. 2007; 67:2187–2196. [PubMed: 17332349]
16. Feldmann G, Habbe N, Dhara S, Bisht S, Alvarez H, Fendrich V, et al. Hedgehog inhibition prolongs survival in a genetically engineered mouse model of pancreatic cancer. Gut. 2008; 57:1420–1430. [PubMed: 18515410]
17. Hidalgo M, Maitra A. The hedgehog pathway and pancreatic cancer. N Engl J Med. 2009; 361:2094–6. [PubMed: 19923581]
18. Nolan-Stevaux O, Lau J, Truitt ML, Chu GC, Hebrok M, Fernàndez-Zapico ME, et al. GLI1 is regulated through Smoothened-independent mechanisms in neoplastic pancreatic ducts and mediates PDAC cell survival and transformation. Genes & development. 2009; 23:24–36. [PubMed: 19136624]
19. Yauch RL, Gould SE, Scales SJ, Tang T, Tian H, Ahn CP, et al. A paracrine requirement for hedgehog signalling in cancer. Nature. 2008; 455:406–10. [PubMed: 18754008]
20. Tian H, Callahan CA, DuPree KJ, Darbonne WC, Ahn CP, Scales SJ, et al. Hedgehog signaling is restricted to the stromal compartment during pancreatic carcinogenesis. PNAS. 2009

21. Olive KP, Jacobetz MA, Davidson CJ, Gopinathan A, McIntyre D, Honess D, et al. Inhibition of Hedgehog signaling enhances delivery of chemotherapy in a mouse model of pancreatic cancer. Science. 2009; 324:1457–61. [PubMed: 19460966]
22. Hwang RF, Moore T, Arumugam T, Ramachandran V, Amos KD, Rivera A, et al. Cancer-associated stromal fibroblasts promote pancreatic tumor progression. Cancer Res. 2008; 68:918–926. [PubMed: 18245495]
23. Bruns CJ, Harbison MT, Kuniyasu H, Eue I, Fidler IJ. In vivo selection and characterization of metastatic variants from human pancreatic adenocarcinoma by using orthotopic implantation in nude mice. Neoplasia. 1999; 1:50–62. [PubMed: 10935470]
24. Yang B, Hird AW, Russell DJ, Fauber BP, Dakin LA, Zheng X, et al. Discovery of novel hedgehog antagonists from cell-based screening: Isosteric modification of p38 bisamides as potent inhibitors of SMO. Medicinal Chemistry Letters. 2012 accepted for publication.
25. Sasaki H, Hui C, Nakafuku M, Kondoh H. A binding site for Gli proteins is essential for HNF-3beta floor plate enhancer activity in transgenics and can respond to Shh in vitro. Development. 1997; 124:1313–22. [PubMed: 9118802]
26. Sasai K, Romer JT, Lee Y, Finkelstein D, Fuller C, McKinnon PJ, et al. Shh pathway activity is down-regulated in cultured medulloblastoma cells: implications for preclinical studies. Cancer Res. 2006; 66:4215–22. [PubMed: 16618744]
27. Chen W, Tang T, Eastham-Anderson J, Dunlap D, Alicke B, Nannini M, et al. Canonical hedgehog signaling augments tumor angiogenesis by induction of VEGF-A in stromal perivascular cells. Proc Natl Acad Sci U S A. 2011; 108:9589–94. [PubMed: 21597001]
28. Liu S, Dontu G, Mantle ID, Patel S, Ahn NS, Jackson KW, et al. Hedgehog signaling and Bmi-1 regulate self-renewal of normal and malignant human mammary stem cells. Cancer Res. 2006; 66:6063–71. [PubMed: 16778178]
29. Bar EE, Chaudhry A, Lin A, Fan X, Schreck K, Matsui W, et al. Cyclopamine-mediated hedgehog pathway inhibition depletes stem-like cancer cells in glioblastoma. Stem Cells. 2007; 25:2524–33. [PubMed: 17628016]
30. Clement V, Sanchez P, de Tribolet N, Radovanovic I, Ruiz i Altaba A. HEDGEHOG-GLI1 signaling regulates human glioma growth, cancer stem cell self-renewal, and tumorigenicity. Curr Biol. 2007; 17:165–72. [PubMed: 17196391]
31. Dierks C, Beigi R, Guo GR, Zirlik K, Stegert MR, Manley P, et al. Expansion of Bcr-Abl-positive leukemic stem cells is dependent on Hedgehog pathway activation. Cancer Cell. 2008; 14:238–49. [PubMed: 18772113]
32. Kikuta K, Masamune A, Watanabe T, Ariga H, Itoh H, Hamada S, et al. Pancreatic stellate cells promote epithelial-mesenchymal transition in pancreatic cancer cells. Biochem Biophys Res Commun. 2010; 403:380–4. [PubMed: 21081113]
33. Tredan O, Galmarini CM, Patel K, Tannock IF. Drug Resistance and the Solid Tumor Microenvironment. Journal of National Cancer Institute. 2007; 99:1441–1454.
34. Sims-Mourtada J, Izzo JG, Ajani J, Chao KS. Sonic Hedgehog promotes multiple drug resistance by regulation of drug transport. Oncogene. 2007; 26:5674–9. [PubMed: 17353904]
35. Queiroz KC, Ruela-de-Sousa RR, Fuhler GM, Aberson HL, Ferreira CV, Peppelenbosch MP, et al. Hedgehog signaling maintains chemoresistance in myeloid leukemic cells. Oncogene. 29:6314–22. [PubMed: 20802532]
36. Chen YJ, Lin CP, Hsu ML, Shieh HR, Chao NK, Chao KS. Sonic hedgehog signaling protects human hepatocellular carcinoma cells against ionizing radiation in an autocrine manner. Int J Radiat Oncol Biol Phys. 80:851–9. [PubMed: 21377281]

STATEMENT OF TRANSLATIONAL RELEVANCE

The Hedgehog (Hh) pathway has emerged as an important pathway in multiple tumor types, including pancreatic cancer (PDAC). Recent evidence suggests that the Hh pathway functions in a paracrine fashion that is dependent on the tumor microenvironment of PDAC. In this study, we determined the role of carcinoma-associated fibroblasts isolated from human pancreatic cancer (pancreatic stellate cells, PSCs) in Hh signaling. The Smoothened (SMO) receptor was highly expressed in PSCs but was absent in pancreatic cancer cells. Activation of the Hh pathway in PSCs resulted in increased cell proliferation which was reversed by a novel SMO inhibitor (AZD8542). *In vivo*, AZD8542 was effective in reducing tumor growth in an orthotopic model of PDAC only when stroma was present, indicating a stroma-dependent paracrine signaling mechanism. Our results suggest that Hh antagonists primarily target the tumor-associated stroma and may be novel therapies for the treatment of pancreatic cancer.

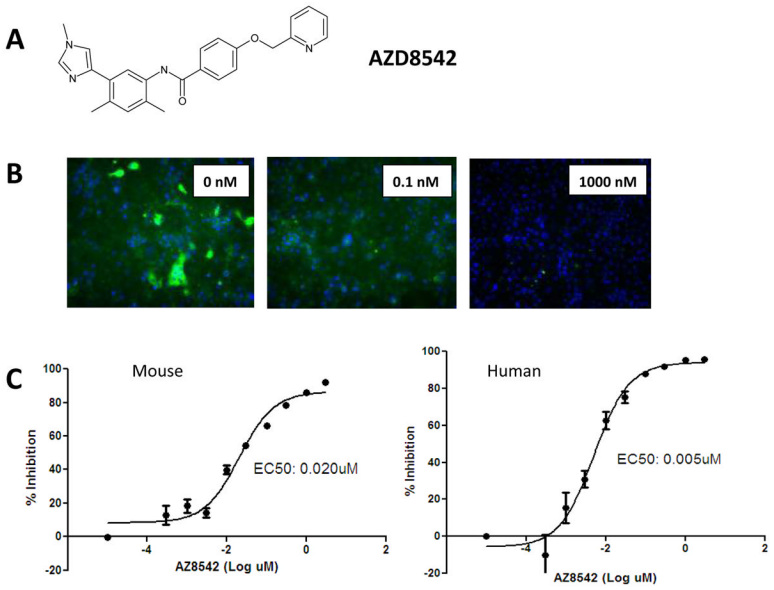

Figure 1.

Identification of a small-molecule SMO inhibitor. (A) Structure of lead compound AZD8542. (B) Treatment of HeLa cells expressing SMO with AZD8542 (0.1 nM and 1000 nM) was able to compete away BODIPY-labeled cyclopamine in a dose-dependent fashion. (C) In the BODIPY-labeled cyclopamine competition assay, affinity of AZD8542 for mouse and human SMO showed similar binding Kd values for both species (mouse, 5nM; human, 20 nM).

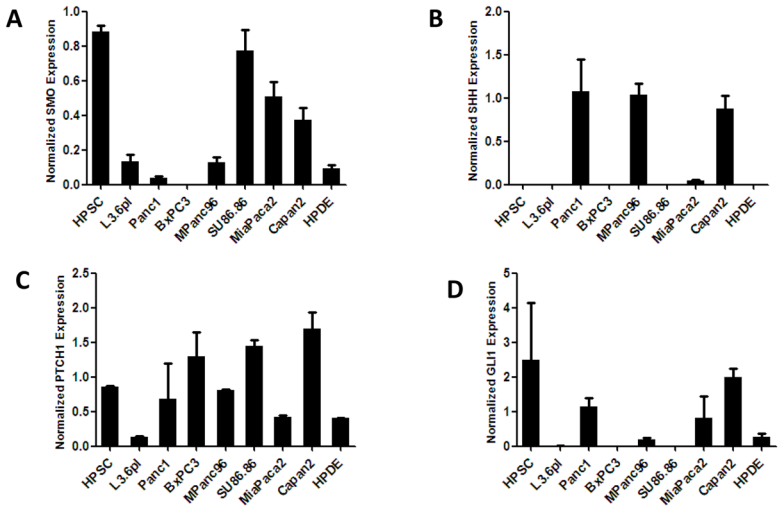

Figure 2.

Hedgehog pathway gene expression. RNA from various pancreas cell lines was analyzed for expression of SMO (A), SHH (B), PTCH1 (C), and GLI1 (D) by qPCR. Expression was normalized to that of the HPRT gene.

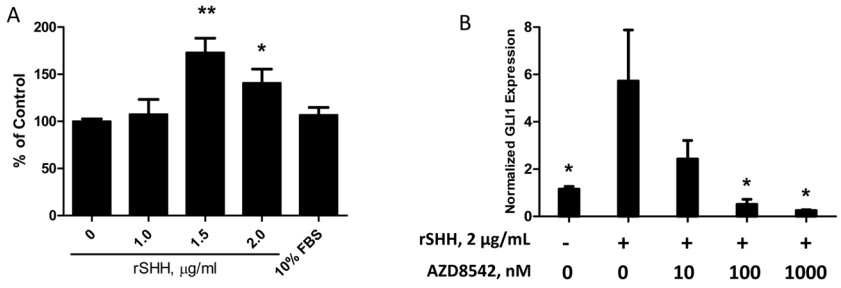

Figure 3.

Stimulation of HPSCs by rSHH induces proliferation and GLI1expression. (A) rSHH (μg/mL) was added to HPSCs grown in 1% DMEM. (A) Proliferation was measured by MTS assay at 72hours. *$p \leq 0.05$, **$p \leq 0.005$ vs. 0 μg/mL rSHH control. (B) HPSCs were treated with rSHH (2 μg/mL) with or without AZD8542. GLI1expression was measured by qPCR and normalized to HPRT. *$p \leq 0.05$ vs.2 μg/mL rSHH, 0nM AZD8542 sample.

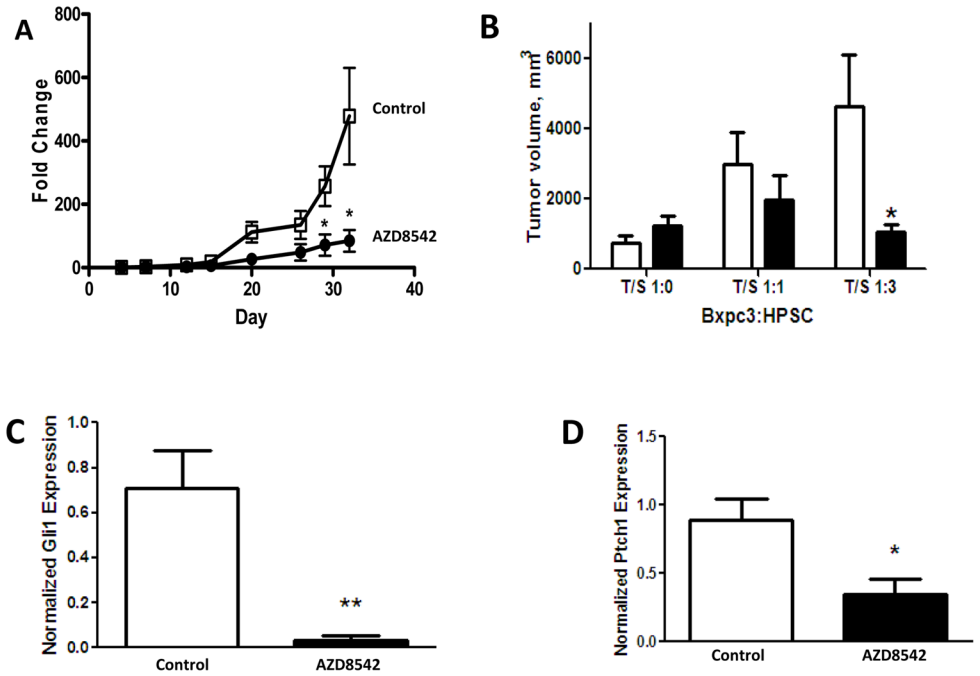

Figure 4.

Effect of AZD8542 in an orthotopic model of pancreatic cancer with luciferase-labeled Bxpc3 cells co-injected with HPSCs. Mice were treated daily with 80mg/kg AZD8542 (black) or vehicle alone (white). (A) Luciferase signal, indicating tumor growth, was measured weekly. (B)Final pancreatic tumor volume was measured after 32 days of drug treatment. (C–D) Expression of downstream targets GLI1and PTCH1wasanalyzed in tumors (T/S ratio 1:3) using qPCR. *$p \leq 0.05$ and **$p \leq 0.005$ vs. vehicle controls.

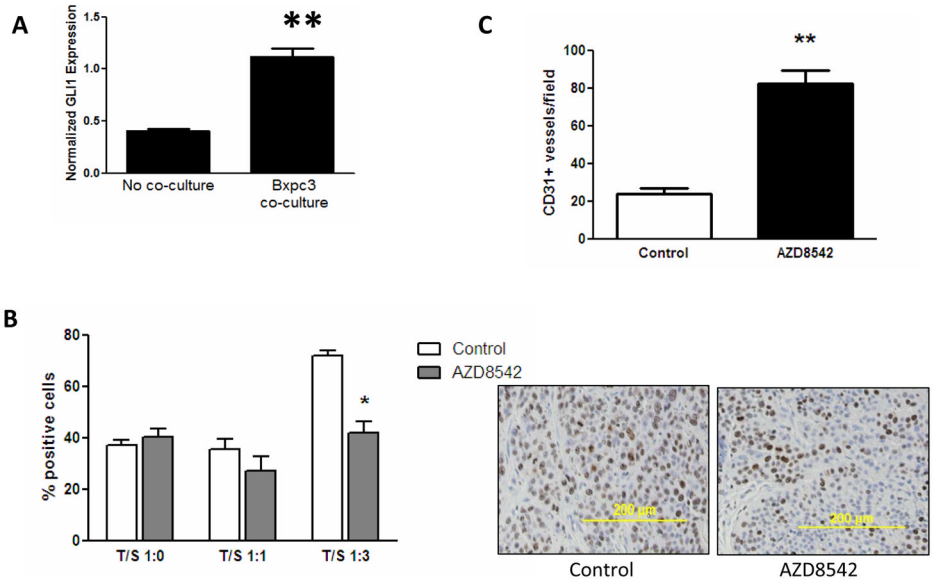

Figure 5.

Hh pathway signaling in PDAC *in vitro* and *in vivo*. (A) Quantitative PCR for Gli1 expression. HPSC-GFP cells were cultured with or without Bxpc3 for 96 hours and sorted by flow cytometry. ** $p<0.0001$. Immunohistochemistry for Ki67 (B) and CD31 (C) was performed on mouse pancreatic tumors with tumor/stroma ratio 1:3 treated with AZD8542 or control. Total magnification 100X. Data is shown as means ± SEM;* $p<0.005$ and ** $p<0.0001$.

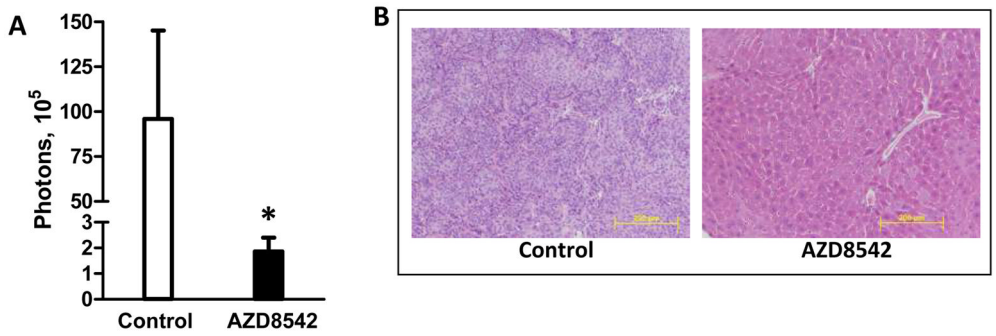

Figure 6.

Effect of AZD8542 on liver metastases in an orthotopic model of pancreatic cancer with luciferase-labeled Bxpc3 cells co-injected with HPSCs. Mice were treated daily with 80mg/kg AZD8542 or vehicle alone. (A)Liver metastases were measured by luciferase signal. (B) Histology was confirmed by H&E staining in mice from the T/S 1:3 group (total magnification 200X). *p=0.06.